Effect of Polymer End Group on the Morphology of Polystyrene/Poly(methyl methacrylate) Composite Particles Prepared by the Solvent Evaporation Method[†]

*Takuya Tanaka, Masaru Okayama, Masayoshi Okubo**

Summary: The effect of polymer end group on the morphology of polystyrene (PS)/poly(methyl methacrylate) (PMMA) composite particles was investigated on the basis of experimental observations and theoretical predictions. Both polymers with potassium persulfate (KPS)-derived hydrophilic end group(s) and 2,2′-azobis(isobutyronitrile) (AIBN)-derived hydrophobic end group(s) were synthesized by emulsifier-free emulsion polymerizations and solution polymerizations, respectively. Composite particles with the same end groups were prepared by release of toluene from PS/PMMA/toluene (1/1/24, w/w/w) droplets dispersed in an aqueous solution of sodium dodecyl sulfate (SDS). At a low SDS concentration, when the polymers with KPS-derived end group(s) were employed, acornlike particles were formed. On the other hand, when the polymers with AIBN-derived end group(s) were used, particles having a dimple were obtained. The interfacial tensions between toluene solutions of the polymers and SDS aqueous medium were lower for KPS-derived end group(s) than for AIBN-derived end group(s), and the difference was much larger for PS phase than PMMA phase. The predicted morphologies obtained from calculation of the minimum total interfacial free energy using the interfacial tensions agreed well with the experimentally observed morphologies in both cases. Moreover, the morphology of PS/PMMA composite particles with different end groups was also examined.

Keywords: colloids; interfacial tension; morphology; phase separation; polymer end group

Introduction

Morphology control of composite polymer particles is of crucial importance for applications in many industrial fields such as coatings, impact modifiers, adhesives, and many other materials. In general, composite polymer particles prepared by various seeded polymerizations have phase-separated structure inside the particle as a result of the incompatibility between seed polymer and polymer formed in the post-polymerization step. The morphology of the composite polymer particles is determined by the competition between thermodynamic and kinetic factors,[1] including the effects of types of polymers, surfactants, monomer concentration in the seed particles, cross-linking density of seed polymer, reaction temperature, and so on.[2–20] Thermodynamic factors favor minimization of the interfacial free energy, whereas kinetic factors (e.g., viscosity in polymerizing particle) hinder it.

The type of initiator for seeded polymerization is also one of the most important factors to determine thermodynamic equilibrium morphology of the resulting particles, because the polar end group of polymer derived from the initiator are

Graduate School of Engineering, Kobe University, Kobe 657-8501, Japan
Tel/Fax: (+81)-78-803-6197;
E-mail: okubo@kobe-u.ac.jp
[†]Part CCCXXVIII of the series ''Studies on Suspension and Emulsion''

Copyright © 2010 WILEY-VCH Verlag GmbH & Co. KGaA, Weinheim

localized at the particle surface and reduce the interfacial tension between the polymer and an aqueous medium.[2,21–28] Therefore, it is necessary to consider the effect of the polar end group (including anchoring effect) on the particle morphology. In a previous study,[2] we examined morphologies of polystyrene (PS)/poly(methyl methacrylate) (PMMA) and PMMA/PS composite particles which were, respectively, prepared by seeded emulsion polymerizations of methyl methacrylate (MMA) with PS seed particles, and styrene (S) with PMMA seed particles, using potassium persulfate (KPS). We clarified that the surface hydrophilicity due to KPS fragments ($-SO_4^-$) at the particle surface, which was estimated by the soap titration method, is one of important factors affecting the particle morphology. Cho and Lee[22] also demonstrated that the anchoring effect on the morphology of PMMA/PS composite particles prepared by seeded emulsion polymerization employing KPS was enhanced by an increase in KPS concentration. The final particle morphology changed from PS-core/PMMA-shell to PMMA-core/PS-shell with increasing amount of KPS-derived end groups on the surface of the PS phase. El-Aasser and coworkers[23] later systematically investigated the morphology prediction of PS/PMMA composite particles prepared by seeded emulsion polymerization using KPS taking into consideration the anchoring effect on the interfacial tension. The predicted morphologies based on minimization of the interfacial free energy were in good agreement with experiment. However, the volume ratio of the polymer formed in the post-polymerization step to the seed polymer continuously increases during seeded emulsion polymerization, and furthermore, the particle morphology undergoes a transition at thermodynamic nonequilibrium as a result of high viscosity in the later stage of polymerization. Therefore, it is instructive to consider the effect of the various factors affecting the particle morphology in simpler systems.

Recently, we have developed morphology control of PS/PMMA (= PMMA/PS) composite particles prepared by slow release of toluene from droplets comprising toluene and previously prepared PS and PMMA (PS/PMMA/toluene = 1/1/24, w/w/w) dispersed in an aqueous solution of surfactants.[29–33] Both polymers were prepared by solution polymerization with 2,2′-azobis(isobutyronitrile) (AIBN) as initiator. Homogeneous PS/PMMA/toluene droplets phase-separated into PS and PMMA phases (containing some toluene) as toluene evaporated. The phase separation proceeded at thermodynamic equilibrium until a polymer weight fraction (w_p) of 0.3 was reached, which represents 80 wt% loss of toluene from the initial composition.[30] Consequently, the final morphology was closely related to the thermodynamic equilibrium morphology of PS/PMMA/toluene droplets. Because of these factors, we attempted to predict the equilibrium morphology of PS/PMMA/toluene droplets ($w_p = 0.17$) based on minimization of the interfacial free energy. It was elucidated that the incorporation of a small amount of PS and PMMA into the PMMA and PS phases significantly affects the interfacial tension between the polymer-toluene and the aqueous phase, and the predicted morphology.[31]

The aim of this article is to clarify the effect of polymer end group as initiator fragment on the PS/PMMA particle morphology reflecting thermodynamic equilibrium morphology of the PS/PMMA/toluene droplet. Furthermore, morphology prediction on the basis of minimizing the interfacial free energy of PS/PMMA/toluene droplets will be discussed.

Experimental Part

Materials

S and MMA were distilled under reduced pressure in a nitrogen atmosphere. Reagent grade 1-pyrenylmethyl methacrylate (PM) (Funakoshi, Tokyo, Japan) was used as a fluorescent moiety of PS without further

Copyright © 2010 WILEY-VCH Verlag GmbH & Co. KGaA, Weinheim

purification. KPS of analytical grade (Nacalai Tesque Inc., Kyoto, Japan) and reagent grade AIBN were purified by recrystallization with water and methanol, respectively. SDS and toluene were used as received from Nacalai Tesque, Inc. Deionized water with a specific resistivity of $5 \times 10^6\,\Omega \cdot \mathrm{cm}$ was used after distillation. All other materials were used as received from Nacalai Tesque, Inc.

Preparation of PS, PMMA and P(S-PM)

Polymers with hydrophilic end group were synthesized by emulsifier-free emulsion polymerizations in a four-necked 1-L round-bottom flask equipped with an inlet of N_2, a reflux condenser, and a half-moon type stirrer under the conditions listed in Table 1. The typical procedure was as follows: Water added to the reactor was heated to 70 °C, and monomer was poured into the reactor. The mixture was deoxygenated with a stream of N_2 for 30 min, and then KPS aqueous solution was added to the reactor. The resulting polymers were dried under vacuum at room temperature, subsequently dissolved in tetrahydrofuran (THF), reprecipitated in methanol, and eventually dried under vacuum at room temperature once again. Solution polymerizations for the synthesis of polymers with hydrophobic end group under the conditions listed in Table 1 were typically performed by as follows: A homogeneous solution of monomer, toluene, and AIBN was charged into glass ampoules, degassed using several N_2/vacuum cycles and sealed off under vacuum. The resulting polymers were reprecipitated in methanol to remove the unreacted monomer and toluene, and subsequently dried under vacuum at room temperature. Number-average molecular weight (M_n) and polydispersity index (PDI) of each polymer are listed in Table 1. S-PM copolymer [P(S-PM) (S/PM = 99.5/0.5, w/w)] with AIBN-derived end groups were prepared under the conditions of our previous article.[30]

Preparation of PS/PMMA Composite Particles

PS/PMMA composite particles were prepared as follows: Toluene solution (0.65 g) of PS and PMMA (PS/PMMA/toluene = 1/1/24, w/w/w) was mixed with aqueous solutions (15 g) of SDS at various concentrations and subsequently stirred vigorously using a NISSEI ABM-2 homogenizer at 4000 rpm for 2 min in a 50-ml glass vial. Toluene was subsequently evaporated from the dispersions stirred with a magnetic stirrer at room temperature for 24 h in the

Table 1.
Preparation of polystyrene (PS) and poly(methyl methacrylate) (PMMA) with KPS-derived and AIBN-derived end group(s) by emulsifier-free emulsion polymerizations[a] and solution polymerizations[b].

Ingredients		PS-K[c]	PMMA-K[d]	PS-A[e]	PMMA-A[f]
S	(g)	18	–	36	–
MMA	(g)	–	18	–	39
KPS	(mg)	90	114	–	–
AIBN	(mg)	–	–	100	100
Toluene	(g)	–	–	24	57
Water	(g)	600	600	–	–
M_n[g] ($\times 10^4$ g · mol^{-1})		5.5	5.5	5.2	6.1
M_w/M_n[h]		3.0	3.5	1.7	1.9

[a] N_2, 70 °C, 24 h, 120 rpm.
[b] N_2, 70 °C, 24 h, 80 cycles/min.
[c] PS with KPS-derived end groups.
[d] PMMA with KPS-derived end group(s).
[e] PS with AIBN-derived end groups.
[f] PMMA with AIBN-derived end group(s).
[g] Number-average molecular weight.
[h] Polydispersity index.
Abbreviations: S, styrene; MMA, methyl methacrylate; KPS, potassium persulfate; AIBN, 2,2′-azobis(isobutyronitrile).

Copyright © 2010 WILEY-VCH Verlag GmbH & Co. KGaA, Weinheim

uncovered glass vial (surface area between dispersion and air was 8 cm^2). The resulting particles were washed with methanol (followed by centrifugation and decantation, repeated three times) to remove excess SDS, and subsequently dried under vacuum at room temperature.

Measurements

The amount of residual toluene in the dispersions was determined by gas chromatography (Shimadzu Corporation, GC-2014) with helium as the carrier gas, and employing *N*,*N*-dimethylformamide as solvent and *p*-xylene as internal standard. Molecular weights were measured by gel permeation chromatography (GPC) with two S/DVB gel columns (TOSOH Corporation, TSK gel GMH_{HR}-H, 7.8 mm i.d. × 30 cm) using THF as eluent at 40 °C at flow rate of 1.0 mL · min^{-1} employing refractive index (TOSOH RI-8020/21) and ultraviolet detectors (TOYO SODA UV-8II). The columns were calibrated with six standard PS samples (1.05×10^3–5.48×10^6, $M_w/M_n = 1.01$–1.15). Polymer compositions in PS and PMMA phases were measured by ^{1}H NMR with a Bruker DPX 250 MHz spectrometer (Karlsruhe, Germany).

Particle Observation

PS/PMMA/toluene droplets and PS/PMMA composite particles were, respectively, observed with a MICROPHOT-FXA optical microscope, a Carl Zeiss Axio Imager. Z1 fluorescence microscope equipped with Apotome (MRm) and a Hitachi S-2460 scanning electron microscope (SEM) at a voltage of 15 kV. To observe the interior of the particles, the dried particles were stained with ruthenium tetraoxide (RuO_4) vapor at room temperature for 30 min in the presence of 1% RuO_4 aqueous solution, embedded in an epoxy matrix, cured at room temperature over night, and subsequently microtomed. The ultrathin cross sections of approximately 100 nm thickness were observed with a JEOL JEM-1230 transmission electron microscope (TEM) at a voltage of 100 kV.

Interfacial Tension Measured by the Pendant Drop Method

A PS/PMMA/toluene (10/10/100, w/w/w) solution was left standing in a graduated cylinder for 5 days and subsequently phase-separated PS-toluene and PMMA-toluene phases were, respectively, removed for further analysis. The density of each solution was measured with a pycnometer (volumetric flask type). Interfacial tensions between the PS-toluene (or PMMA-toluene) and aqueous solutions at various SDS concentrations were measured by the pendant drop method with a Drop Master 500 (Kyowa Interface Science Co., Ltd., Japan). All of the measurements were performed at room temperature (ca. 20 °C). The accuracy of the interfacial tensions reported was ± 0.1 mN/m.

Interfacial Tension Measured by the Spinning Drop Method

Interfacial tension between PS-toluene and PMMA-toluene solutions was measured by the spinning drop method with a Site100 (Krüss, Germany) at 20 °C. A drop of the PS-toluene solution was suspended in the PMMA-toluene solution and made to rotate at 9000 rpm in a horizontal tube, and the diameter was measured. The accuracy of the interfacial tensions was ± 0.01 mN/m.

Results and Discussion

PS and PMMA with KPS-derived hydrophilic end group(s) ($-SO_4^-$), denoted PS-K and PMMA-K, were synthesized by emulsifier-free emulsion polymerizations, and AIBN-derived hydrophobic end group(s) ($-C(CH_3)_2CN$), denoted PS-A and PMMA-A, were synthesized by solution polymerizations. Figure 1 shows SEM photographs of PS-K/PMMA-K and PS-A/PMMA-A composite particles prepared by release of toluene from polymer/toluene droplets dispersed in aqueous solutions of SDS at various concentrations. No effect of the particle size on the structure was observed. The structures of PS-K/PMMA-K

Copyright © 2010 WILEY-VCH Verlag GmbH & Co. KGaA, Weinheim

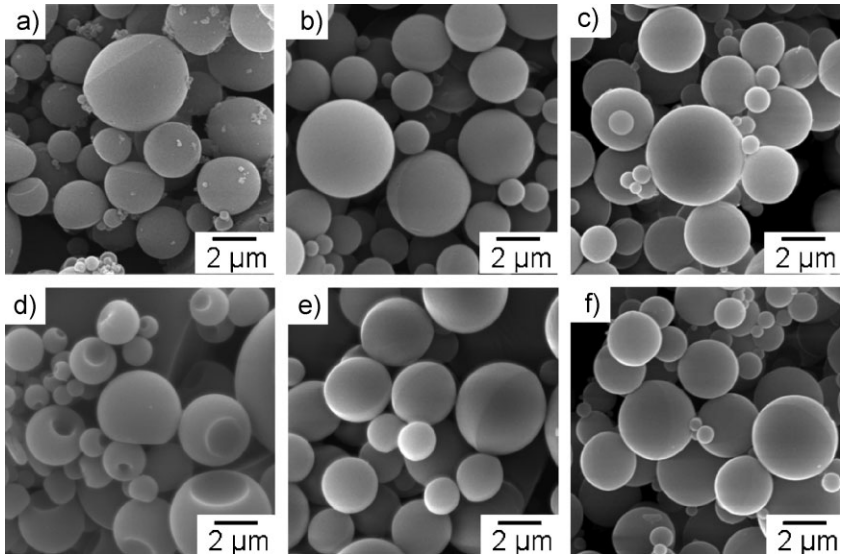

Figure 1.
SEM photographs of PS-K/PMMA-K (a, b, c) and PS-A/PMMA-A (d, e, f) (1/1, w/w) composite particles prepared by evaporation of toluene from polymer/toluene (1/12, w/w) droplets dispersed in SDS aqueous solution. SDS concentrations ($g \cdot L^{-1}$): (a, d) 0.33; (b, e) 1.3; (c, f) 3.3.

particles were acornlike at $0.33\,g \cdot L^{-1}$ SDS aqueous solution and spherical at 1.3 and $3.3\,g \cdot L^{-1}$ SDS aqueous solutions. On the other hand, PS-A/PMMA-A particles had a dimple on the surface, acornlike and spherical structures at 0.33, 1.3 and $3.3\,g \cdot L^{-1}$ SDS aqueous solutions, respectively. Acornlike and dimple structures of the particle were attributed to the volume reduction of the PS phase after hardening of the PMMA phase during toluene releasing from the corresponding droplets.[30]

Figure 2 shows TEM photographs of ultrathin cross sections of RuO_4-stained PS-K/PMMA-K and PS-A/PMMA-A composite particles at various SDS concentrations. RuO_4 stains PS but not PMMA, thus PS and PMMA phases appear dark and light, respectively.[34] The morphologies of the particles were closely correlated with the particle structures as shown in Figure 1. At $0.33\,g \cdot L^{-1}$ SDS aqueous solution, remarkably different morphologies of the PS-K/PMMA-K and PS-A/PMMA-A particles were observed, although the PS phase was engulfed by the PMMA phase in both cases. The morphology difference might be attributed that the influence of the hydrophilic KPS-derived end group(s) on the interfacial tensions between polymers-toluene phases and SDS aqueous solution becomes pronounced at a low SDS concentration. In other words, the effect of hydrophilic polymer end group(s) on the interfacial tension progressively weakens with increasing SDS concentration, and as a result the difference of the particle morphology became smaller. The particle morphology reflects thermodynamic equilibrium morphology of phase-separated polymers/toluene droplets. Therefore, the morphologies of polymers/toluene droplets at $0.33\,g \cdot L^{-1}$ SDS aqueous solution were observed by optical and fluorescence microscope.

P(S-PM) with AIBN-derived end groups [P(S-PM)-A] was synthesized by solution copolymerization. However, P(S-PM) with KPS-derived end groups could not be synthesized by emulsifier-free emulsion copolymerization because of the hydrophobicity of PM. Therefore, the small amount of P(S-PM)-A was added with

Copyright © 2010 WILEY-VCH Verlag GmbH & Co. KGaA, Weinheim

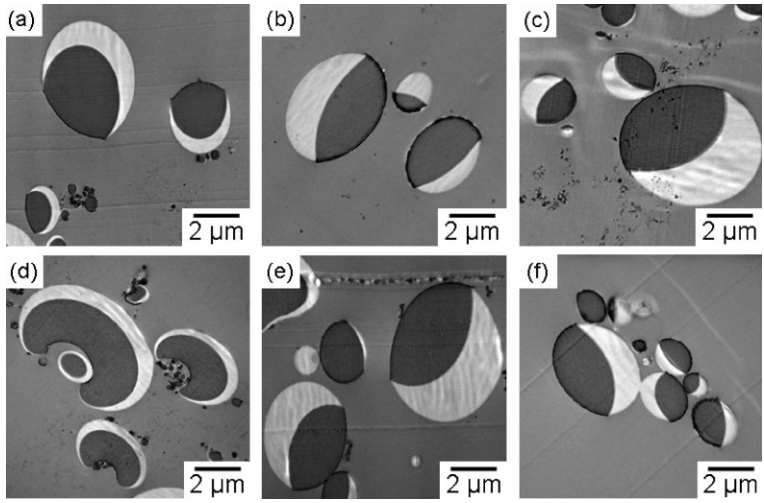

Figure 2.
TEM photographs of ultrathin cross sections of RuO_4-stained PS-K/PMMA-K (a, b, c) and PS-A/PMMA-A (d, e, f) (1/1, w/w) composite particles prepared by evaporation of toluene from polymer/toluene (1/12, w/w) droplets dispersed in SDS aqueous solution. SDS concentrations ($g \cdot L^{-1}$): (a, a') 0.33; (b, b') 1.3; (c, c') 3.3.

keeping the ratio of PS/P(S-PM)/PMMA = 0.75/0.25/1.0 (w/w/w) to distinguish the PS phase. P(S-PM) (S-PM = 99.83–0.17, mol-mol) would be preferentially located in the PS phase, and would not affect the droplet morphology.

Figure 3 shows optical and fluorescence micrographs of toluene droplets containing dissolved PS-K/(P(S-PM)-A)/PMMA-K and PS-A/(P(S-PM)-A)/PMMA-A at $w_p = 0.17$ dispersed in $0.33\,g \cdot L^{-1}$ SDS aqueous solution. A PS-rich phase appears light, and a PMMA-rich phase does dark. The interfacial area between PS*-K-toluene phase and aqueous medium was larger than that between PS*-A-toluene phase and aqueous medium, where asterisks mean that each polymer phase contains small amount of the other polymer with the same kind of end group (i.e. PS-K solution contains PMMA-K and vice versa)[31]. KPS-derived hydrophilic end group(s) might reduce the interfacial tensions between ''both'' polymer-toluene phases and the aqueous medium.

The thermodynamic equilibrium morphology of the droplets was determined by the minimization of the total interfacial free energy. The total interfacial free energy change is expressed as

$$\Delta G = \sum \gamma_i A_i - \gamma_0 A_0 \quad (1)$$

where γ_i is the interfacial tension of the ith interface and A_i is the corresponding

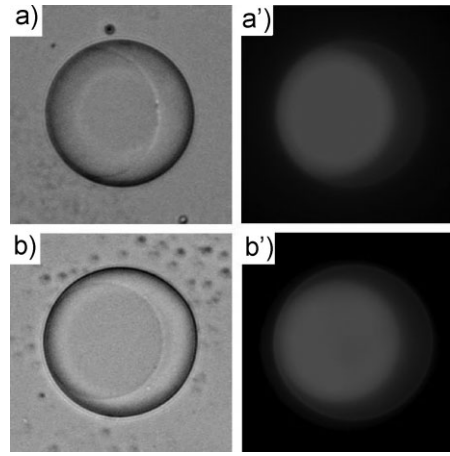

Figure 3.
Optical (a, b) and fluorescence (a', b') micrographs of toluene droplets containing dissolved PS-K/PMMA-K (1/1, w/w) (a), PS-K/P(S-PM)-A/PMMA-K (0.75/0.25/1.0, w/w/w) (a'), PS-A/PMMA-A (1/1, w/w) (b), and PS-A/P(S-PM)-A/PMMA-A (0.75/0.25/1.0, w/w/w) (b') at $w_p = 0.17$ dispersed in $0.33\,g \cdot L^{-1}$ SDS aqueous solutions.

Copyright © 2010 WILEY-VCH Verlag GmbH & Co. KGaA, Weinheim

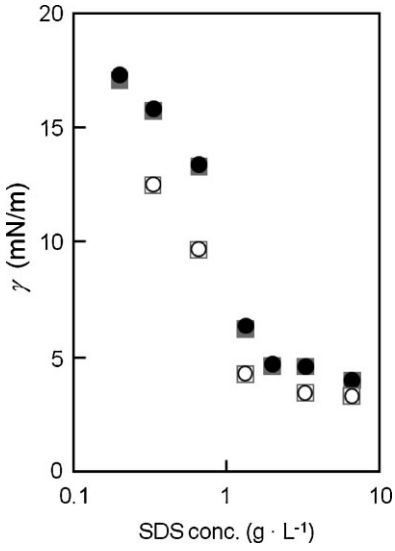

Figure 4.
Interfacial tensions between the polymer phases and SDS aqueous solutions as functions of SDS concentration. PS*-K (○) and PMMA*-K (□) phases, and PS*-A (●) and PMMA*-A (■) phases were, respectively, obtained from phase-separated PS-K/PMMA-K/toluene and PS-A/PMMA-A/toluene (1/1/10, w/w/w) solutions.

interfacial area.[14–17,23,24,31,35] In the present system, the droplet has three interfaces: the PS*-toluene phase/aqueous medium, the PMMA*-toluene/aqueous medium, and PS*-toluene/PMMA*-toluene phases. To calculate ΔG, each interfacial tension was measured in both cases.

Figure 4 shows the interfacial tensions (pendant drop method) between PS*-K, PMMA*-K, PS*-A, and PMMA*-A-toluene droplets and SDS aqueous solutions, which are, respectively, denoted $\gamma_{\text{PS*-K-T/SDS aq.}}$, $\gamma_{\text{PMMA*-K-T/SDS aq.}}$, $\gamma_{\text{PS*-A-T/SDS aq.}}$, and $\gamma_{\text{PMMA*-A-T/SDS aq.}}$, as functions of SDS concentration. $\gamma_{\text{PS*-K-T/SDS aq.}}$ and $\gamma_{\text{PMMA*-K-T/SDS aq.}}$ were, respectively, lower than $\gamma_{\text{PS*-A-T/SDS aq.}}$ and $\gamma_{\text{PMMA*-A-T/SDS aq.}}$ over the entire range of SDS concentration, and got closer with increasing SDS concentration. Moreover, the difference between $\gamma_{\text{PS*-A-T/SDS aq.}}$ and $\gamma_{\text{PS*-K-T/SDS aq.}}$ was slightly larger than that between $\gamma_{\text{PMMA*-A-T/SDS aq.}}$ and $\gamma_{\text{PMMA*-K-T/SDS aq.}}$ (although it is too complicated to decipher absolute values of interfacial tension from Figure 4). This result might be attributed that the hydrophobic PS-toluene phase is more susceptible to the hydrophilic KPS-derived end group than relatively hydrophilic PMMA-toluene phase. This result would explain that the interfacial area between PS*-K-toluene phase and the aqueous medium was larger than that between PS*-A-toluene phase and the aqueous medium as shown in Figure 3.

Based on the above results, it would appear that PS-K/PMMA-A and PS-A/PMMA-K particles have the morphology with larger interfacial area between polymer-K phase and aqueous medium compared to PS-A/PMMA-A particles, because the interfacial tension between polymer-K-toluene phase and aqueous medium is lower than that between polymer-A-toluene phase and aqueous medium.

Figure 5 shows SEM photographs of PS-K/PMMA-A and PS-A/PMMA-K composite particles, and TEM photographs of ultrathin cross sections of RuO_4-stained particles, and Figure 6 indicates optical and fluorescence micrographs of toluene droplets containing dissolved PS-K/(P(S-PM)-A)/PMMA-A and PS-A/(P(S-PM)-A)/PMMA-K at $w_p = 0.17$ dispersed in $0.33\,g \cdot L^{-1}$ SDS aqueous solution. In the case of PS-K/PMMA-A composite particles, the acornlike morphology was observed, and the interfacial area between PS-K and the aqueous medium was larger for PS-K/PMMA-A/toluene droplets than PS-A/PMMA-A/toluene droplets. However, PS-A/PMMA-K composite particles did not exhibit the excentered core-shell, but the acornlike morphology contrary to expectation. The interfacial area between PMMA-K phase and the aqueous medium was lower for PS-A/PMMA-K/toluene droplets than PS-A/PMMA-A/toluene droplets. This will be discussed later. The total interfacial free energy change has to be taken into account when considering thermodynamic equilibrium morphology. To calculate ΔG (Equation 1) in both cases, each interfacial tension is required.

Copyright © 2010 WILEY-VCH Verlag GmbH & Co. KGaA, Weinheim

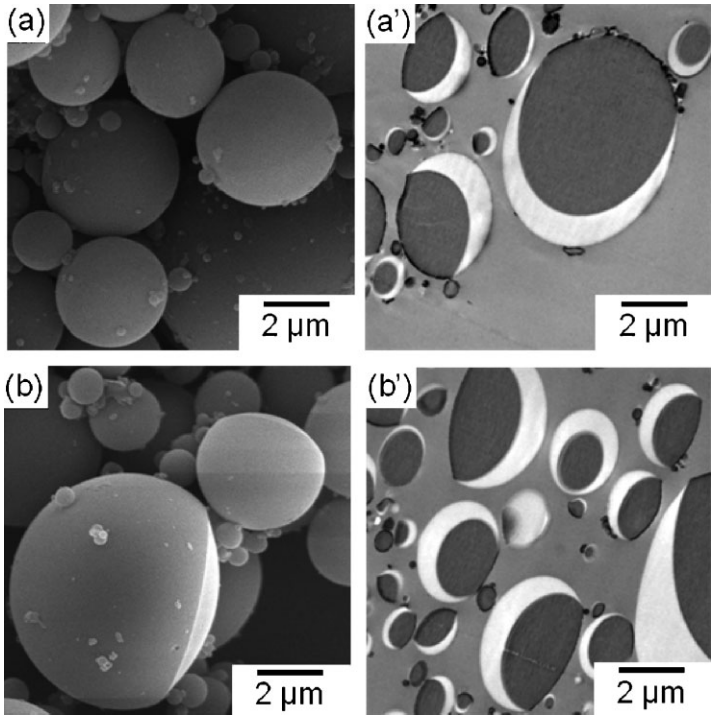

Figure 5.
SEM photographs (a, b) of PS-K/PMMA-A (a, a') and PS-A/PMMA-K (b, b') (1/1, w/w) composite particles prepared by evaporation of toluene from polymer/toluene (1/12, w/w) droplets dispersed in $0.33\,g \cdot L^{-1}$ SDS aqueous solution, and TEM photographs (a', b') of ultrathin cross sections of RuO_4-stained particles.

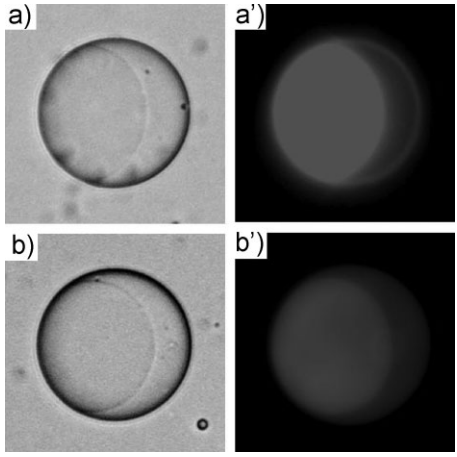

Figure 6.
Optical (a, b) and fluorescence (a', b') micrographs of toluene droplets containing dissolved PS-K/PMMA-A (1/1, w/w) (a), PS-K/P(S-PM)-A/PMMA-A (0.75/0.25/1.0, w/w/w) (a'), PS-A/PMMA-K (1/1, w/w) (b), and PS-A/P(S-PM)-A/PMMA-K (0.75/0.25/1.0, w/w/w) (b') at $w_p = 0.17$ dispersed in $0.33\,g \cdot L^{-1}$ SDS aqueous solutions.

Figure 7 shows the interfacial tension measured with the pendant drop method between PS**-K, PMMA**-A, PS**-A, and PMMA**-K-toluene droplets and SDS aqueous solutions, which are, respectively, denoted $\gamma_{PS^{**}\text{-K-T/SDS aq.}}$, $\gamma_{PMMA^{**}\text{-A-T/SDS aq.}}$, $\gamma_{PS^{**}\text{-A-T/SDS aq.}}$, and $\gamma_{PMMA^{**}\text{-K-T/SDS aq.}}$, as functions of SDS concentration, where double asterisks mean that the polymer phase contains a small amount of the other polymer with different kinds of end group. Not only $\gamma_{PS^{**}\text{-K-T/SDS aq.}}$ and $\gamma_{PMMA^{**}\text{-K-T/SDS aq.}}$ but also $\gamma_{PS^{**}\text{-A-T/SDS aq.}}$ and $\gamma_{PMMA^{**}\text{-A-T/SDS aq.}}$ were, respectively, lower than $\gamma_{PS^{*}\text{-A-T/SDS aq.}}$ and $\gamma_{PMMA^{*}\text{-A-T/SDS aq.}}$. This would be due to the incorporation of a small amount of hydrophilic polymer-K into the other hydrophobic polymer-A phase. Therefore, molar ratios of PS to PMMA in the phase-separated PS/PMMA/toluene (1/1/10, w/w/w) were, respectively, measured to be 1:0.294 and 0.185:1 (PS-A/

Copyright © 2010 WILEY-VCH Verlag GmbH & Co. KGaA, Weinheim

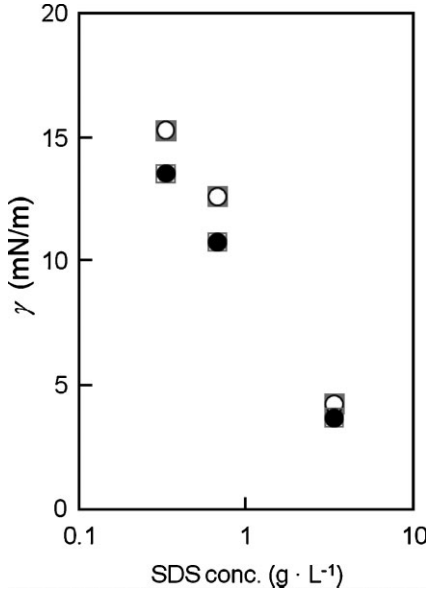

Figure 7.
Interfacial tensions between the polymer phases and SDS aqueous solutions as functions of SDS concentration. PS**-K (○) and PMMA**-A (■) phases, and PS**-A (●) and PMMA**-K (□) phases were, respectively, obtained from phase-separated solutions of PS-K/PMMA-A/toluene and PS-A/PMMA-K/toluene (1/1/10, w/w/w) solutions.

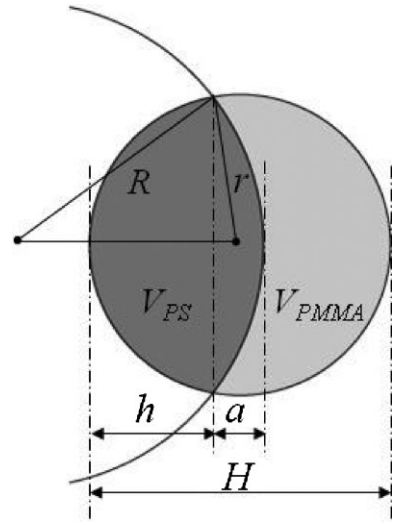

Figure 8.
Cross-sectional image of PS/PMMA/toluene droplet after phase separation.

PMMA-A),[31] 1:0.095 and 0.226:1 (PS-K/PMMA-K), 1:0.113 and 0.207:1 (PS-K/PMMA-A), and 1:0.073 and 0.171:1 (PS-A/PMMA-K). From these results, it can be concluded that the hydrophilic polymer-K incorporated into the other hydrophobic polymer-A phase adsorbs at the interface, resulting in a reduction in the interfacial tension between polymer-A-toluene phase and aqueous medium as well as that between polymer-K-toluene phase and aqueous medium. In other words, the interfacial tension between both polymer-toluene phases and aqueous medium is dominated by the hydrophilic polymer end group when droplets include the polymer with hydrophilic end group.

According to our previous study,[31] thermodynamic equilibrium morphology of the droplets ($w_p = 0.17$) dispersed in $0.33\,g \cdot L^{-1}$ SDS aqueous medium was predicted based on Equation 1 using experimental interfacial tensions. The geometry was applied as shown in Figure 8. Thus, Equation 1 can be rewritten as

$$\begin{aligned}\Delta G = {} & \gamma_{PS-T/SDSaq.} 2\pi r h \\ & + \gamma_{PMMA-T/SDSaq.} 2\pi r (H - h) \\ & + \gamma_{PS-T/PMMA-T} 2\pi R a \\ & - \gamma_{PS,PMMA-T/SDSaq.} 4\pi R_0^2 \end{aligned} \quad (2)$$

where $\gamma_{\text{PS-T/PMMA-T}}$ denotes the interfacial tension between PS-toluene and PMMA-toluene phases, and $\gamma_{\text{PS,PMMA-T/SDS aq.}}$ is the interfacial tension between PS/PMMA/toluene solution (before phase separation) and SDS aqueous medium. The parameters r, h, H, R and a are defined in Figure 8, and R_0 denotes the radius of the droplet before phase separation. If all the interfacial tensions and volume ratio of PS-toluene phase to PMMA-toluene phase (V_{PS}/V_{PMMA}) are known, it is possible to calculate ΔG as functions of h and H. $\gamma_{\text{PS-T/SDS aq.}}$ and $\gamma_{\text{PMMA-T/SDS aq.}}$, in Equation 2 were, respectively, obtained from Figures 4 and 7. $\gamma_{\text{PS-T/PMMA-T}}$ in Equation 2 was measured by the spinning drop method (0.015 mN/m). V_{PS}/V_{PMMA} values in all

Copyright © 2010 WILEY-VCH Verlag GmbH & Co. KGaA, Weinheim

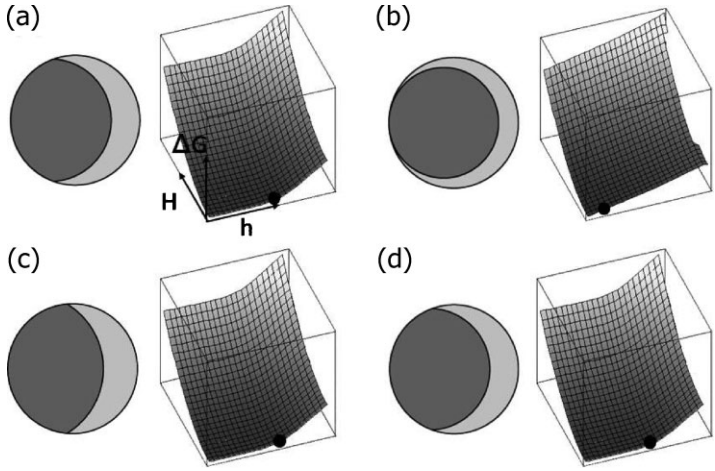

Figure 9.
Graphic display of the predicted morphologies of PS-K/PMMA-K/toluene (a), PS-A/PMMA-A/toluene (b), PS-K/PMMA-A/toluene (c), and PS-A/PMMA-K/toluene (d) droplets ($w_p = 0.17$) dispersed in $0.33\,g \cdot L^{-1}$ SDS aqueous solution. Dark region denotes PS phase containing toluene.

cases were measured, which were approximately 1.5.

Figure 9 shows a graphic display of the predicted morphology of PS-K/PMMA-K/toluene, PS-A/PMMA-A/toluene, PS-K/PMMA-A/toluene and PS-A/PMMA-K/toluene droplets dispersed in $0.33\,g \cdot L^{-1}$ SDS aqueous solution. The predicted morphologies were in good agreement with the experimentally observed morphologies in all cases. Consequently, the morphology of composite polymer particles reflecting thermodynamic equilibrium morphology of the droplets can also be predicted. It would be a useful tool to predict the particle morphology when polymerization using hydrophilic initiator is carried out.

Figure 10 shows optical micrograph and SEM photograph of PS-K^+/PMMA-K^+ composite particles and TEM photographs of ultrathin cross sections of RuO_4-stained composite particles, prepared using polymers with KPS-derived end group(s) before purification by reprecipitation using THF/methanol (polymer-K^+). As seen in SEM photograph (Figure 10b), some particles had a large dimple at the surface, others seemed spherical, although all PS-K/PMMA-K (after purification) composite particles prepared under the same SDS

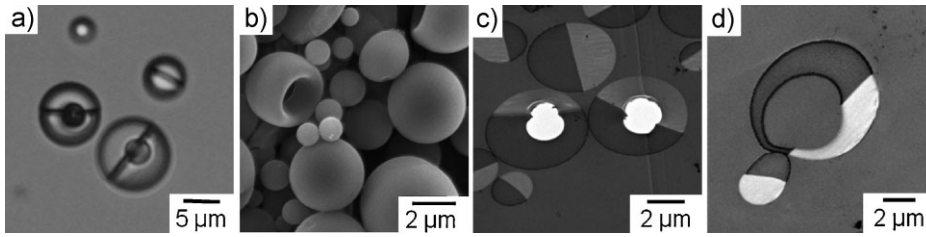

Figure 10.
Optical micrograph (a) and SEM photograph (b) of PS-K^+/PMMA-K^+ (1/1, w/w) composite particles prepared by evaporation of toluene from polymer/toluene (1/12, w/w) droplets dispersed in $3.3\,g \cdot L^{-1}$ SDS aqueous solution, and TEM photographs (c, d) of ultrathin cross sections of RuO_4-stained composite particles. (c) and (d) are only on different visual fields.

Copyright © 2010 WILEY-VCH Verlag GmbH & Co. KGaA, Weinheim

concentration were spherically shaped (Figure 1c). In the TEM photographs, some particles had a hole not filled with epoxy resin (Figure 10c), others had one filled with it (Figure 10d). Considering that all holes of the dimple particles (Figure 2d) were filled with epoxy resin, it would appear that there are not only particles having a large dimple but also particles with a hollow structure, thus resulting in the contrast difference in the optical micrograph (Figure 10a). Tauer[36] demonstrated that hydrophilic polymer end groups buried inside particles may gather in a particular spot and water accumulates there, and suggested larger particles and lower M_n facilitate preparation of particles with hollow structure due to accumulated water. We also reported the preparation of submicrometer-sized multihollow PS particles by seeded emulsion polymerization of S using KPS with PS seed particles with incorporated nonionic emulsifier.[37] Buried sulfate end groups inside the PS particles are one of important factors for formation of multihollow structure.[38] In the present study, larger particles had a tendency to have a hollow structure. M_n and PDI of PS and PMMA before purification were, respectively, lower (5.2×10^4 and $3.8 \times 10^4\,g \cdot mol^{-1}$) and higher (3.2 and 4.6) than those after purification (see Table 1). This suggests that low molecular weight PS-K^+ and PMMA-K^+ buried inside the particles induces water absorption into the particles during toluene evaporation. Further investigations are currently underway to clarify these points.

Conclusion

The effect of polymer end group on the morphology of PS/PMMA (1/1, w/w) composite particles prepared by evaporation of toluene from PS/PMMA/toluene (1/1/24, w/w/w) droplets dispersed in an aqueous solution of SDS has been demonstrated. At a low concentration of SDS, KPS-derived hydrophilic polymer end group(s) greatly affected the morphology of the droplet in which PS and PMMA phase-separated, resulting in acornlike particles. On the other hand, the particles had a dimple at the surface when both polymers with AIBN-derived end group(s) were employed. This is attributed to KPS-derived polymer end group(s) reducing the interfacial tension between hydrophobic PS-toluene phase and aqueous medium slightly more than that between relatively hydrophilic PMMA-toluene phase and aqueous medium. PS/PMMA particles with the end groups of different combinations exhibited acornlike shapes in both cases. This might be due to preferential adsorption of the polymer with KPS-derived end group(s) over the other polymer with AIBN-derived end group(s) phase at the interface. Predicted thermodynamic equilibrium morphologies of the droplets obtained from calculation of the minimum total interfacial free energy agreed well with those experimentally observed. These findings are of importance for morphology control of composite particles prepared by multistage polymerization employing hydrophilic initiator.

Acknowledgements: This work was supported by Grant-in-Aid for Scientific Research (Grant 21245050) from the Japan Society for the Promotion of Science (JSPS).

[1] D. C. Sundberg, Y. G. Durant, *Polym. React. Eng.* **2003**, *11*, 379.
[2] M. Okubo, A. Yamada, T. Matsumoto, *J. Polym. Sci. Polym. Chem. Ed.* **1980**, *16*, 3219.
[3] M. Okubo, Y. Katsuta, T. Matsumoto, *J. Polym. Sci. Polym. Lett. Ed.* **1980**, *18*, 481.
[4] M. Okubo, M. Ando, A. Yamada, Y. Katsuta, T. Matsumoto, *J. Polym. Sci. Polym. Lett. Ed.* **1981**, *19*, 143.
[5] M. Okubo, Y. Katsuta, T. Matsumoto, *J. Polym. Sci. Polym. Lett. Ed.* **1982**, *20*, 45.
[6] D. I. Lee, T. Ishikawa, *J. Polym. Sci. Polym. Chem. Ed.* **1983**, *21*, 147.
[7] T. I. Min, A. Klein, M. S. El-Aasser, J. W. Vanderhoff, *J. Polym. Sci. Polym. Lett. Ed.* **1983**, *21*, 2845.
[8] V. Dimonie, M. S. El-Aasser, A. Klein, J. W. Vanderhoff, *J. Polym. Sci. Polym. Chem. Ed.* **1984**, *22*, 2197.
[9] S. Muroi, H. Hashimoto, K. Hosoi, *J. Polym. Sci. Polym. Chem. Ed.* **1984**, *22*, 1365.

Copyright © 2010 WILEY-VCH Verlag GmbH & Co. KGaA, Weinheim

[10] M. P. Merkel, V. L. Dimonie, M. S. El-aasser, J. W. Vanderhoff, *J. Polym. Sci. Part A: Polym. Chem.* **1987**, *25*, 1755.
[11] M. Okubo, *Makromol. Chem., Macromol. Symp.* **1990**, *35/36*, 307.
[12] H. R. Sheu, M. S. El-Aasser, J. W. Vanderhoff, *J. Polym. Sci. Part A: Polym. Chem.* **1990**, *28*, 629.
[13] H. R. Sheu, M. S. El-Aasser, J. W. Vanderhoff, *J. Polym. Sci. Part A: Polym. Chem.* **1990**, *28*, 653.
[14] D. C. Sundberg, A. P. Casassa, J. Pantazopoulos, M. R. Muscato, *J. Appl. Polym. Sci.* **1990**, *41*, 1425.
[15] Y.-C. Chen, V. L. Dimonie, M. S. El-Aasser, *J. Appl. Polym. Sci.* **1992**, *45*, 487.
[16] C. L. Winzor, D. C. Sundberg, *Polymer* **1992**, *33*, 3797.
[17] C. L. Winzor, D. C. Sundberg, *Polymer* **1992**, *33*, 4269.
[18] V. L. Dimonie, E. S. Daniels, O. L. Shaffer, M. S. El-Aasser, ''*Emulsion polymerization and emulsion polymers*'', P. A. Lovell, M. S. El-Aasser, Eds., Wiley, New York 1997, Chapter 9, pp 293.
[19] O. Karlsson, H. Hassander, B. Wesslen, *J. Appl. Polym. Sci.* **1997**, *63*, 1543.
[20] P. Rajatapiti, V. L. Dimonie, M. S. El-Aasser, M. S. Vratsanos, *J. Appl. Polym. Sci.* **1997**, *63*, 205.
[21] T. Matsumoto, M. Okubo, T. Imai, *Kobunshi Ronbunshu* **1975**, *32*, 229.
[22] I. Cho, K.-W. Lee, *J. Appl. Polym. Sci.* **1985**, *30*, 1903.
[23] Y.-C. Chen, V. L. Dimonie, M. S. El-Aasser, *J. Appl. Polym. Sci.* **1991**, *42*, 1049.
[24] J.-E. Jonsson, H. Hassander, B. Tornell, *Macromolecules* **1994**, *27*, 1932.
[25] M. Okubo, Y. Konishi, H. Minami, *Colloid Polym. Sci.* **2001**, *279*, 519.
[26] J. E. Jonsson, O. J. Karlsson, H. Hassander, B. Tornell, *Macromolecules* **2001**, *34*, 1512.
[27] J. M. Stubbs, D. C. Sundberg, *J. Appl. Polym. Sci.* **2004**, *91*, 1538.
[28] P. Sun, Y. Li, S. Sun, K. Zhao, *Polymer Bulletin* **2005**, *55*, 323.
[29] M. Okubo, N. Saito, T. Fujibayashi, *Colloid Polym. Sci.* **2005**, *283*, 691.
[30] N. Saito, Y. Kagari, M. Okubo, *Langmuir* **2006**, *22*, 9397.
[31] N. Saito, Y. Kagari, M. Okubo, *Langmuir* **2007**, *23*, 5914.
[32] N. Saito, R. Nakatsuru, Y. Kagari, M. Okubo, *Langmuir* **2007**, *23*, 11506.
[33] T. Tanaka, R. Nakatsuru, Y. Kagari, N. Saito, M. Okubo, *Langmuir* **2008**, *24*, 12267.
[34] J. S. Trent, J. I. Scheinbeim, P. R. Couchman, *Macromolecules* **1983**, *16*, 589.
[35] S. Torza, S. G. Mason, *J. Colloid Interface Sci.* **1970**, *33*, 67.
[36] K. Tauer, *Macromolecules* **2006**, *39*, 2007.
[37] M. Okubo, H. Kobayashi, T. Matoba, Y. Oshima, *Langmuir* **2006**, *22*, 8727.
[38] H. Kobayashi, E. Miyanaga, M. Okubo, *Langmuir* **2007**, *23*, 8703.

Copyright © 2010 WILEY-VCH Verlag GmbH & Co. KGaA, Weinheim